

Selective Laser Sintering and Reaction Sintering of Ceramic Composites

P. Kamatchi Subramanian, Guisheng Zong and H.L. Marcus
Center for Materials Science and Engineering
The University of Texas at Austin
Austin, TX 78712.

Abstract

Selective Laser Sintering and Reaction Sintering (SLS and SLRS) are used as methods of forming composites and preforms. $\text{Al}_2\text{O}_3/\text{Al}$ and SiC/Al were studied as model systems. Ceramic and metallic powders are mixed and locally sintered using SLS and SLRS. Post processing heat treatment was also employed. Wettability and residual stress aspects of this process are discussed.

Introduction

Composite materials consisting of a polymer or a metal matrix reinforced with a strengthening phase started developing in the early 1960's. The reinforcement can be as particulate or as fibers. While these composite materials show great promise of improved strength and stiffness, fabrication of parts from the metal and ceramic matrix composites has limited their application.

One of the methods of overcoming the processing difficulties is to form preforms from the reinforcing phase in the required shape and then to infiltrate the preforms with matrix material. Selective Laser Sintering (SLS) and Selective Laser Reaction Sintering (SLRS) offer the possibility of forming netshape preforms which could then be infiltrated. In the SLS or SLRS of preforms or composites described here, the reinforcing ceramic phase, is mixed with the metal and locally sintered under the laser beam. The metal melts and binds the ceramic together into a porous composite. In SLRS part of the metal powder reacts with the oxygen in the atmosphere to form an oxide. Prior work on the Selective Laser Sintering of ceramics at University of Texas involved binding the ceramic with a low melting temperature inorganic binder^{1,2}. The issues involved in SLS and SLRS of metal and ceramic composites are examined in this paper. The material systems examined in this work are $\text{Al}_2\text{O}_3/\text{Al}$ and SiC/Al .

Experimental

$\text{Al}_2\text{O}_3/\text{Al}$

Powders of Al_2O_3 (15 μ spherical) and Al (20 μ spherical) were mixed in various ratios by weight and sintered in a SLS system^{3,4} under the 100W Nd:YAG laser (1.06 μm) modulated at 20KHz. Single layer tests were conducted on these powders using various power levels and scan speeds. From these measurements the scanning speeds and power levels used in the study were determined. Multilayered parts were made using the powder delivery and leveling systems in the SLS chamber^{3,4}. No powder bed biasing temperature was employed during the process. Three compositions containing 15%, 25% and 35% by weight of Al were made and sintered.

During sintering under the laser beam of the $\text{Al}_2\text{O}_3/\text{Al}$ system, part of the Al melts and partially oxidizes as it binds the particles together. The untransformed Al is further

transformed to the oxide by means of a secondary heat treatment. The part was heated in a furnace under air to a temperature of 1050°C for 18 hours and then furnace cooled.

SiC/Al

SiC powder (15 μ) and Al powder (20 μ) were mixed in the ratio 3:1 and sintered in the 1.1kW CO₂ Laser (10.6 μ m) SLS system. This material system could not be sintered in the 100W SLS system because the laser power was not sufficient . The part was then fired at 1300°C in air to partially oxidize the aluminum.

Results of SLS and SLRS of Al₂O₃/Al composites.

It was found that 30-35W of laser power is sufficient to sinter the 25 and 35 wt% of Al while about 43W of power was required to sinter the 15wt % of Al. In order to have a proper basis for comparison all specimens for density measurement were made with 43W of laser power and at a scan speed of 4.6 cm/sec.

Micro structure

Both the surface and cross-section of the Al₂O₃ /Al composite prior to secondary treatment were observed in a Scanning Electron Microscope (SEM). The molten Al has wet the alumina particles and is bonding the particles together (Fig.1). Regions appear as agglomerates of high density (Fig.2). The regions of high density are separated by regions where the particles are only loosely bound (Fig.3). In this region the Al₂O₃ particles are not completely wet by the Al.

The distance of separation between the agglomerates decreases as the percentage of metal in the powder mixture increases. This may be seen by comparing Fig.1 which is from a part made out of 85:15 Al₂O₃: Al mixture and Fig.4 . which is from a part of 65:35 mixture where the agglomeration covers most of the surface. The cross section of the specimen after firing in air has similar agglomeration (Fig.5). The agglomerated region is a fairly dense dispersion of the Al₂O₃ in the Al matrix. (Fig.6)

Density measurements

Specimens of 2.5cmX2.5cm cross-section with varied thickness of approximately 7 to 9mm were made and density was determined by a direct volume measurement both before and after firing. The variation in density with composition is shown in Fig.7. The density decreases with increase in the composition of Al. This is because of the lower density of Al. (Density of Al =2.7g/cc , density of Al₂O₃ = 3.97g/cc) This is modified by the fraction of Al that is reaction sintered. The fraction of full theoretical density of this composite always remained around 0.45 . A line corresponding to 45% of the theoretical density of the composite with weight percentage of Al is also plotted on Fig.7 . This seems to indicate that the composite density reflects the powder bed density.

Mechanical properties

25 Wt% Al specimens of 0.6cmx7.6cmx2.5cm were sintered and fired. Four point bend strength tests were conducted at room temperature in air at 0.2mm/min on these. The average bend strength for the 25 wt% Al composition was determined to be 3.6 \pm 0.7 MPa (520 \pm 100 psi) . Five samples were measured.

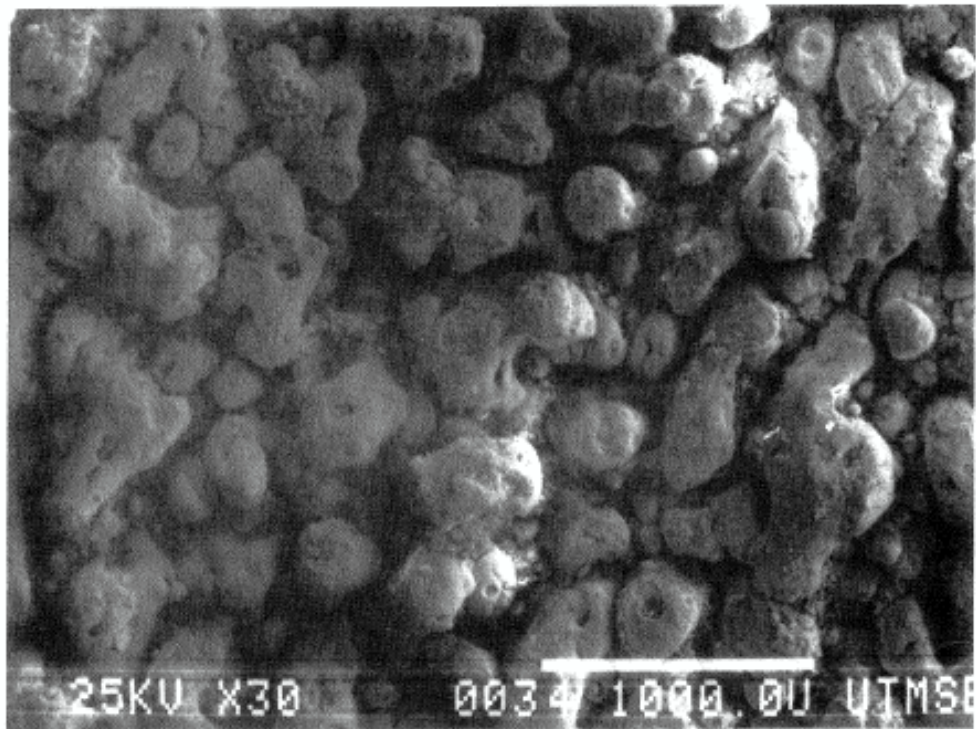
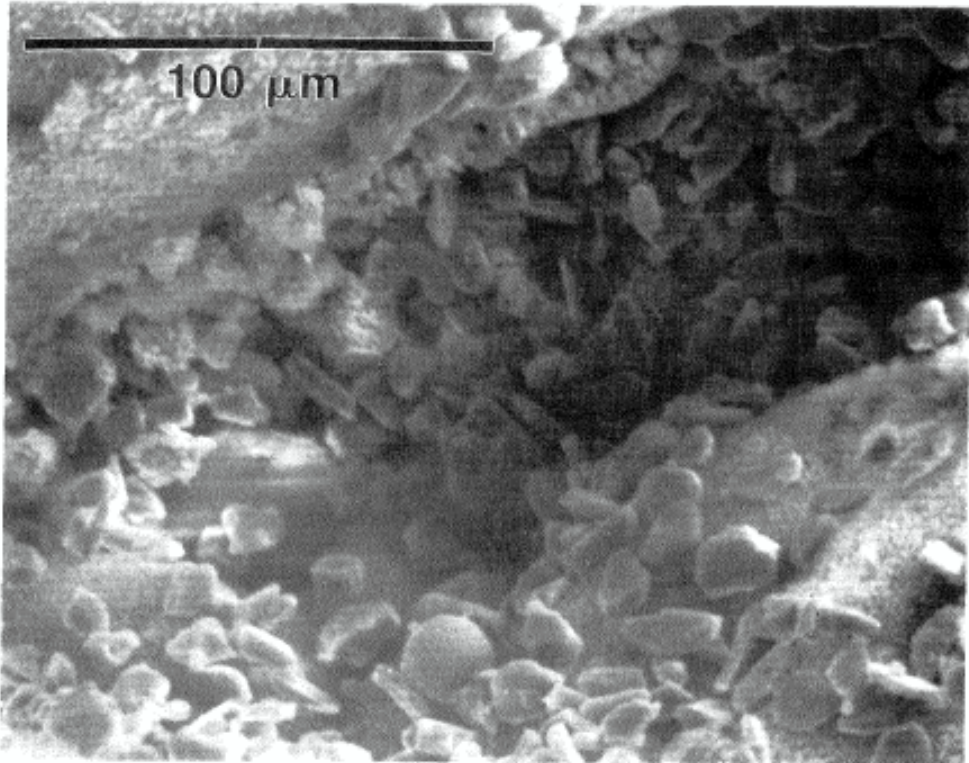


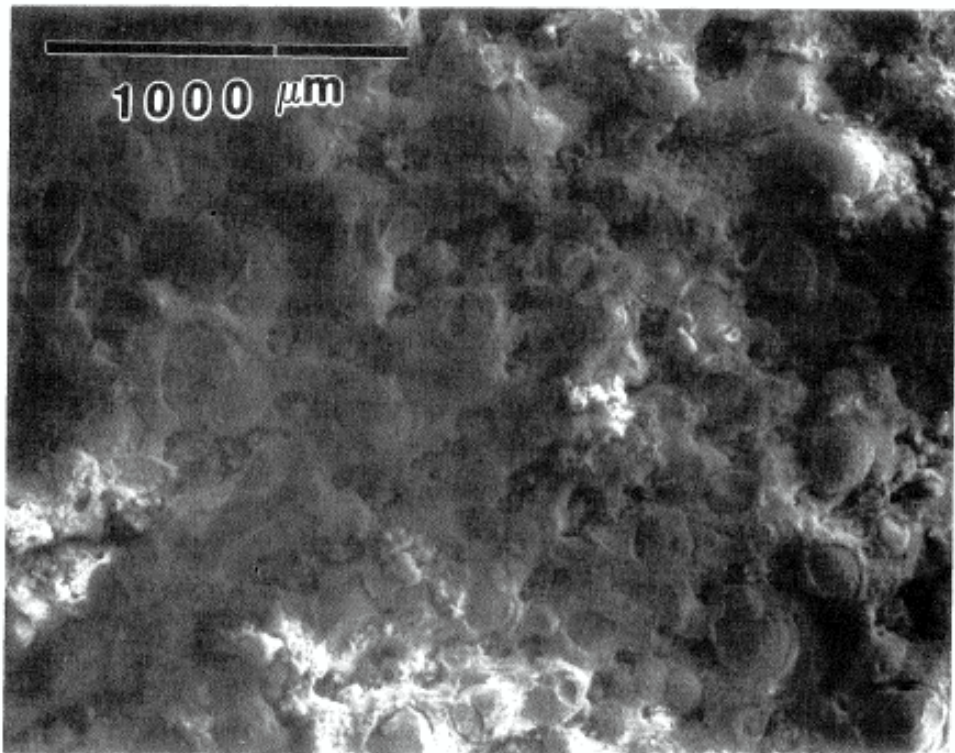
Figure1. Surface of a composite containing 15 % Al. Agglomerates and regions of low density may be seen.



Figure 2. An enlarged view of an agglomerated region. It may be seen that these regions are very dense.



**Figure 3. A view of one of the low density regions
It may be seen that the powder particles are
not enveloped by a dense metallic layer.**



**Figure 4. Surface of a composite containing 35% metal..
The denser agglomerates are closer spaced.**

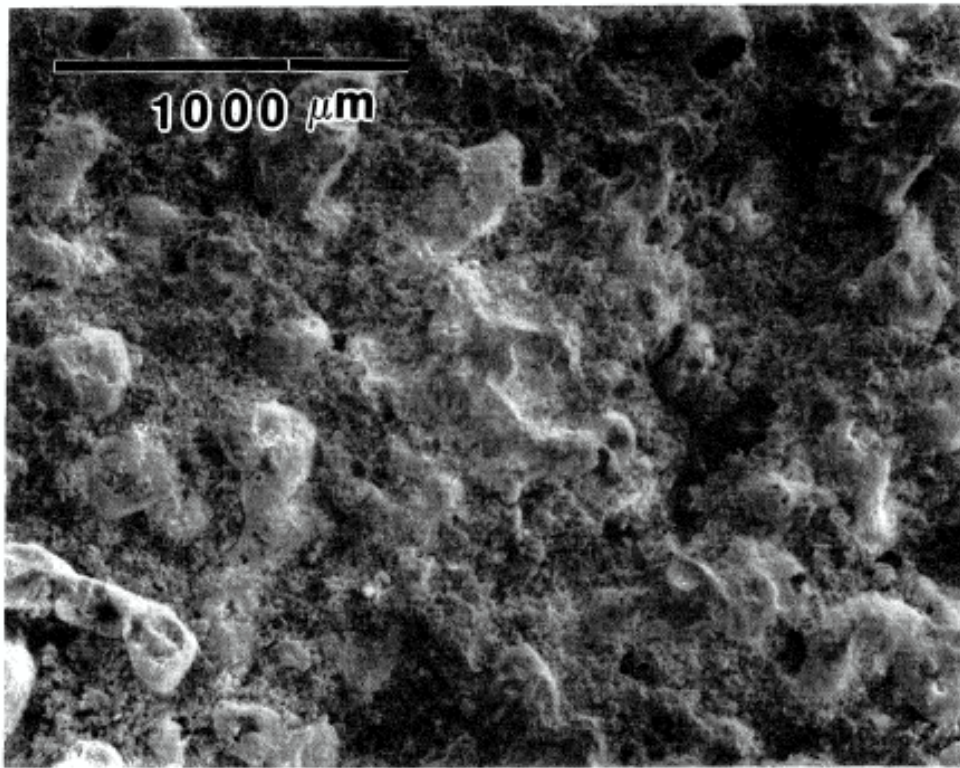


Fig. 5 Cross-section of a 75:25 specimen .
It is similar to the surface of the specimen.

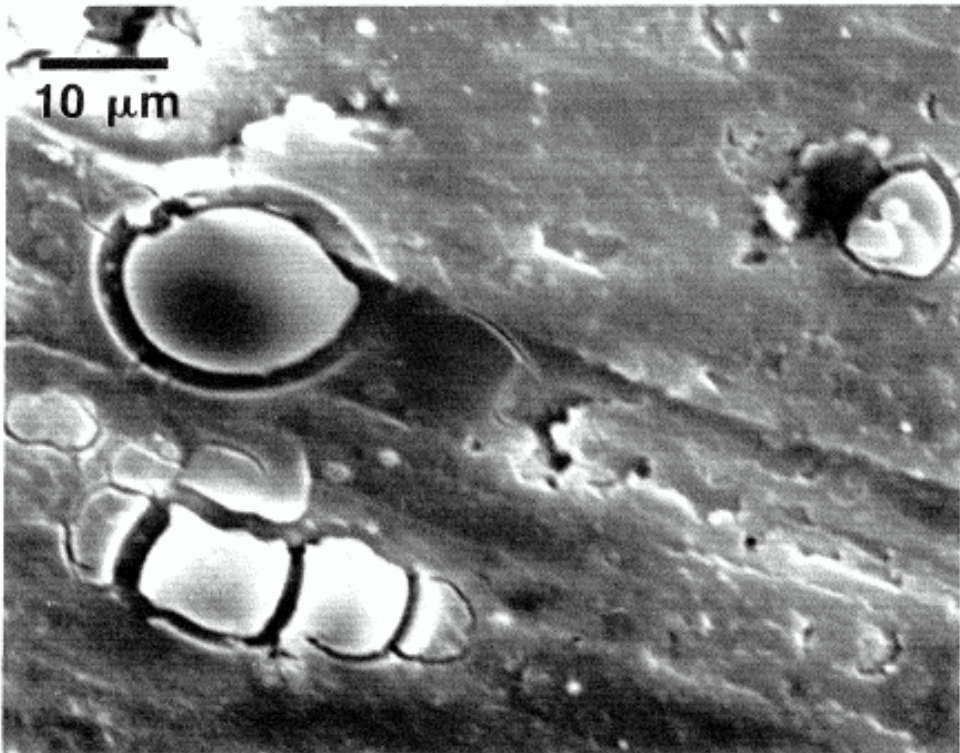


Figure.6. Cross-section through an agglomerate. The Alumina particles are surrounded by a matrix of Aluminum.

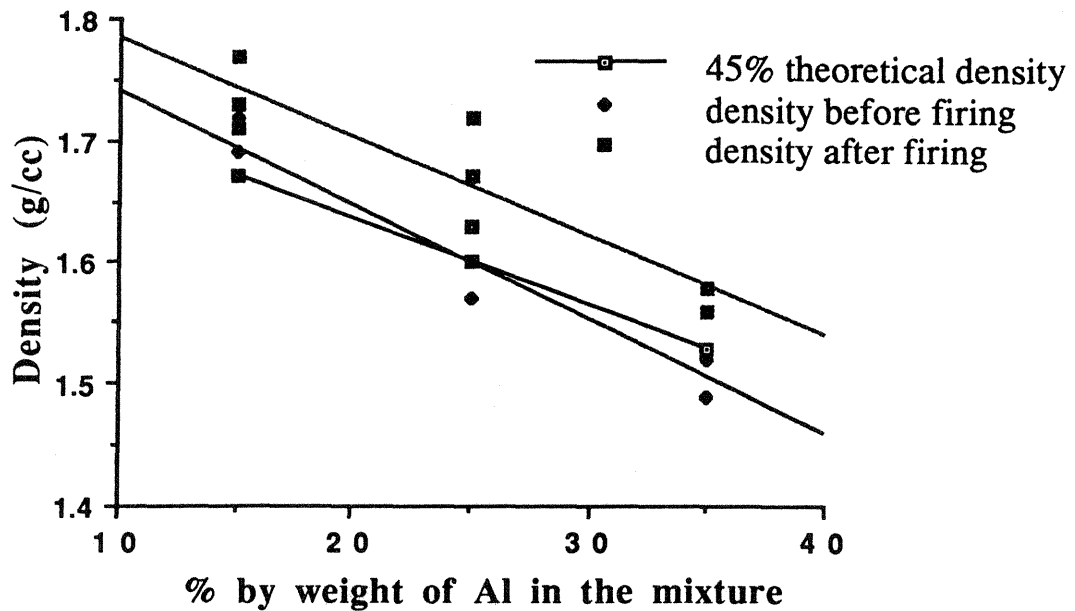


Figure 7. Variation of density with weight percentage of Aluminum.

Results of the SLS and SLRS of SiC/Al composites.

SiC powder (15μ) and Al powder (20μ) were mixed in the ratio 3:1 and sintered in the high power workstation under the 1.1 kW CO₂ laser. A power level of 120W and a scan speed of 1.66cm/s was employed. The part was then fired at 1300°C in air for 18 hours and furnace cooled. The fired density was 1.3g/cc which is 0.42 of the theoretical density. X-ray diffraction shows that the phases present are SiC, Al and α -Al₂O₃. A picture of a part formed is shown in Fig.8. This shows that shapes of SiC/Al/Al₂O₃ can be made by this process.

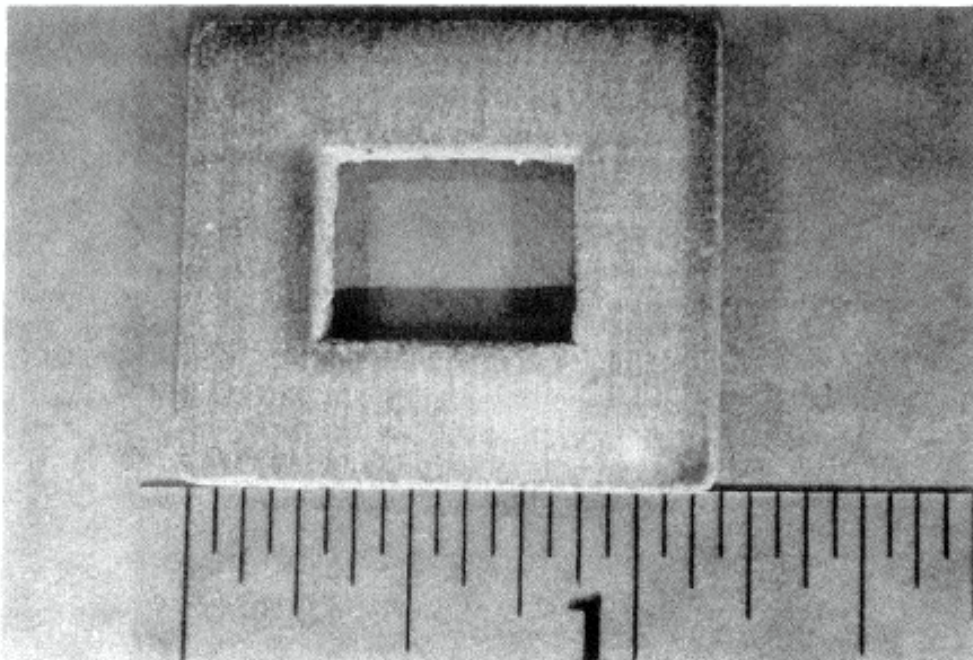


Figure.8. A SiC/Al part.

Discussion

The agglomerated regions in the $\text{Al}_2\text{O}_3/\text{Al}$ composite are where the Al has completely wet the Al_2O_3 . The wettability is normally characterized in terms of the wetting angle. Lower wetting angle implies better wetting of the ceramic by the metal phase. The wetting angle changes with temperature. In the case of $\text{Al}_2\text{O}_3/\text{Al}$ the wetting angle changes with temperature as given by Table I⁵

Table I

Temperature	Contact angle
700	120
800	110
900	90
1000	75

Hence in order to obtain good binding between the Al_2O_3 ceramic and the Al matrix phase it is not only necessary to melt Al but also to heat it to a sufficiently high temperature to reduce the wetting angle. This would imply having a high power of the laser beam. Preheating the powder allows lower laser power to raise the temperature to aid wetting. Wetting agents may also be added. The effect of the wetting agents is to reduce the wetting angle and thus help in densification but none were added in this study.

In the case of SiC/Al systems the variation in wetting angle is given in Table II⁶. It can be seen that this requires the Al to be heated to a higher temperature than the $\text{Al}_2\text{O}_3/\text{Al}$ system. Hence the higher power to sinter the SiC/Al system.

Table II

Temperature	Contact angle
725	150
900	130
1000	90

Residual stresses.

The powder in this process is at room temperature. When the laser scans the surface the metal is heated to a temperature of at least 660°C (the melting point of Al) and higher to get wetting. The metal melts, wets the Ceramic and binds it together. The composite also undergoes rapid cooling due to the surrounding cool material. The coefficient of thermal expansion of the Al ($23\text{-}33 \times 10^{-6}/^\circ\text{C}$)⁷ over the temperature range 25 to 500°C is much greater than the SiC ($5 \times 10^{-6}/^\circ\text{C}$)⁷ or Al_2O_3 ($7 \times 10^{-6}/^\circ\text{C}$)⁷ causing it to shrink more than SiC or Al_2O_3 with cooling. The constraint on the shrinkage due to the ceramic results in development of very local residual stresses across the metal ceramic interface. Another cause of residual stress is the temperature gradient along the scan line. In this case the coefficient of expansion can be calculated by the rule of mixtures such that, $\alpha_{\text{composite}} = \alpha_{\text{Al}}V_{\text{Al}} + \alpha_{\text{Al}_2\text{O}_3}V_{\text{Al}_2\text{O}_3}$ where V_{Al} and $V_{\text{Al}_2\text{O}_3}$ are the volume fractions of Al and Alumina respectively. The solid state cooling in the cold surrounding material leads to a more global residual stress pattern.

The problems associated with residual stress increases with increase in percentage of metal due to the increase in the coefficient of expansion. Increase in power has been observed to aggravate the residual stress probably due to the increased temperature gradient along the scan line. Fig.9 shows the debonding between SLS layers of the

$\text{Al}_2\text{O}_3/\text{Al}$ composite when the penetration depth combined with the resulting residual stress is not taken into account.

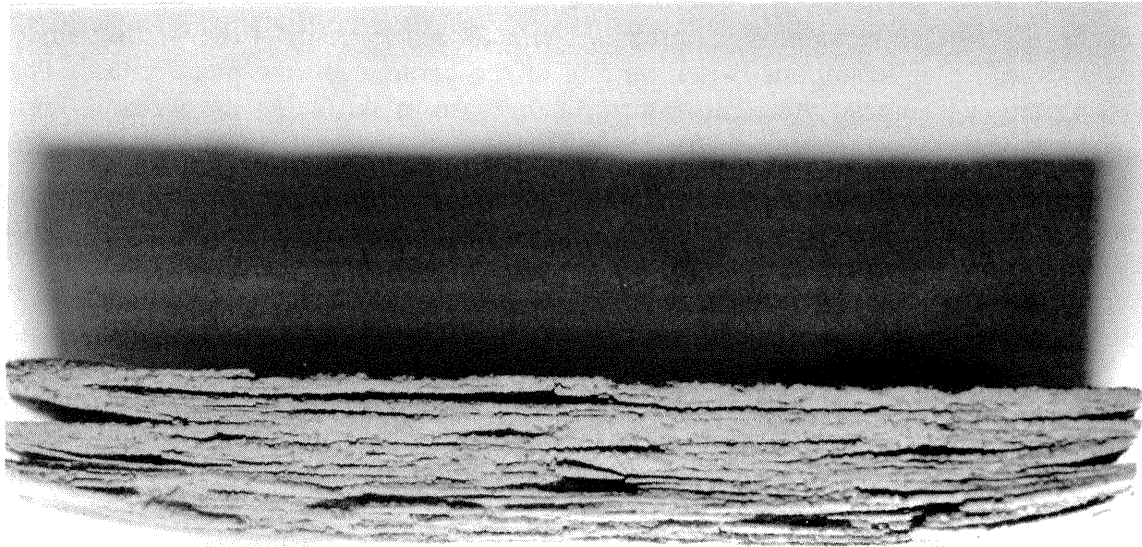


Figure 9. Cracks that occur in a specimen on account of residual stresses

Summary and Future Research.

Selective Laser Sintering and Reaction sintering show promise to be viable methods to form ceramic composites and preforms of $\text{Al}_2\text{O}_3/\text{Al}$ and SiC/Al . Future work will be to determine the effects of varying particle size ratios and the effect of wetting agents. In addition the influence of preheating the powder on residual stress and mechanical properties will be studied.

References.

1. U. Lakshminarayan , S. Ogrydziak and H.L. Marcus, "Selective Laser sintering of ceramic materials ", Proceedings of the solid Freeform fabrication symposium , Ed. J.J. Beaman, H.L. Marcus, D.L. Bourell and J.W. Barlow, 1990, pp. 16 .
2. U. Lakshminarayan and H.L. Marcus, Microstructural and Mechanical properties of $\text{Al}_2\text{O}_3/\text{P}_2\text{O}_5$ and $\text{Al}_2\text{O}_3/\text{B}_2\text{O}_3$ by Selective Laser Sintering", Proceedings of the solid freeform fabrication symposium, Ed. H.L. Beaman, J.W. Barlow, D.L. Bourell and R.H. Crawford, 1991, p.205
3. C. Deckard and J.J.Beaman, Proceedings, 15th conference on Production research and Technology, University of California at Berkeley, 1989, p.623
4. C. Deckard, Selective Laser Sintering, Ph.D. Dissertation , The University of Texas at Austin, December 1988.

5. D.A. Weirauch, Jr. "A reappraisal of wetting in the system Al-Al₂O₃ from 750 - 1000°C ", Ceramic micro structures 86 Role of interfaces edited by J. A. Pask and A. G. Evans p.329
6. C. A. Calow and A. Moor , in "Practical Metallic Composites " , The Institution of Metallurgists, London, 1974, p.B17.
7. CRC handbook of tables for applied engineering science, second edition, 1980, p.249.

Acknowledgement.

This research was supported by NSF under grant number DDM 8914212.